Int. J. Electrochem. Sci., 11 **(2016)** 5952 – 5961, doi: 10.20964/2016.07.16

International Journal of ELECTROCHEMICAL SCIENCE
www.electrochemsci.org

Electrochemical Determination of Imidacloprid in Soil Sample Based on Photosynthesized Silver Nanoparticles from *Hypnea musciformis*

Ganggang Pan[1,*], *Jing Chen*[1] *and Jianfang Guang*[2]

[1] Key Lab Efficient Irrigation and Drainage & Agricultural Soil and Water Environment, Ministry of Education, Hohai University, Nanjing, 210098, Jiangsu, P.R. China
[2] Collage of Water Conservancy & Hydropower, Hohai University, Nanjing, 210098, Jiangsu, P.R. China
[*]E-mail: pgg999@hhu.edu.cn

Received: 25 March 2016 / *Accepted:* 22 April 2016 / *Published:* 4 June 2016

In this communication, we proposed an eco-friendly chemical route for photosynthesizing silver nanoparticles (Ag NPs) using the extract of red alga *Hypnea musciformis* extract. The biosynthesized Ag NPs were characterize using SEM, UV-vis spectroscopy, XRD and FTIR. Further study showed the biosynthesized Ag NPs can be applied for electrode surface modification and used for electrocatalytic determination of imidacloprid in the soil sample.

Keywords: *Hypnea musciformis*; Ag NPs; Biosynthesis; Photosynthesis; Pesticide; Imidacloprid

1. INTRODUCTION

Over the past two decades, nanoscience and nanotechnology received considerable attentions. The fundamental part of the nanotechnology is production of desired nanostructures [1]. The nanomaterials is a terminology of the material at least has one dimension in the size range from 1 to 100 nm. Various materials with different morphology were synthesized by researchers. Among them, metallic nanomaterial have attracted lots attention in many research fields due to their intrinsic properties compared with that of their bulk status [2]. The mechanical, physical and chemical properties of the metallic nanomaterials can be altered by their individual size, size distribution, dispersion status and surface area. Especially, metallic nanomaterials commonly have high specific surface area to volume ratio, which is favourable for many applications such as catalysis, adsorption,

sensor fabrication and anti-bacterial property [3]. So far, many metallic nanostructures such as gold [4], platinum [5], palladium [6, 7], silver [8], copper [9], can be synthesized using well developed chemical routes.

For Ag NPs, many different Ag based nanoparticles were prepared using physical [10], chemical [11] and biological processes [12], including Ag NPs, AgCl NPs [13] and the Ag/AgCl NPs composite [14]. Currently, physical and chemical routes are commonly used for these nanoparticles preparation. However, the physical approach usually needs sophisticated instruments and the chemical method involves toxic reagents. Therefore, developing an eco-friendly and cost effective method for Ag NPs preparation is essential for further exploring their applications.

Green biosynthesis of Ag NPs represents an alternative approach to substitute chemical and physical method. So far, several reports demonstrated the successful synthesis of Ag NPs using biological agents such as leaf extract, fungi and bacterial. For example, Sathyavathi and co-workers demonstrated the successful formation of Ag NPs using *Coriandrum sativum* leaf extract and the biosynthesized Ag NPs was used for nonlinear optics [15]. Veerasamy and co-workers reported the successful synthesis of Ag NPs using mangosteen leaf extract and evaluated its antimicrobial activities [16]. Kalishwaralal and co-workers demonstrated the formation of Ag NPs using a bacterium, *Brevibacterium casei* [17]. Verma et al. [18] reported the synthesis of Ag NPs using an endophytic fungus *Aspergillus clavatus*.

Seaweeds have been found in many potential applications such as antiviral [19], cytotoxic [20], antispasmodic [21], antibacterial [22] and insecticidal properties [23]. Marine red alga *Hypnea musciformis* is one of the ecologically important alga, commonly existing in tide pools and on rocky intertidal benches. Here, the extract of the *Hypnea musciformis* has been tested for their ability to produce Ag NPs by reducing the precursor $AgNO_3$ without adding other reagents. The biosynthesized Ag NPs was characterized using UV-vis spectroscopy, SEM, FTIR and XRD. Moreover, the biosynthesized Ag NPs were used for electrode surface modification and applied for electrochemical determination of imidacloprid (N-{1-[(6-Chloro-3-pyridyl)methyl]-4,5-dihydroimidazol-2-yl}nitramide) in soil samples.

2. EXPERIMENTS

2.1. Materials

Red algae *Hypnea musciformis* was collected from Nanjing Botanical Garden. Fresh *Hypnea musciformi* sample was washed with ethanol and water to remove the impurity. Drying process was carried out at an oven with 80^{o}C overnight. After drying, the *Hypnea musciformis* was chopped into small pieces and then smashed using a blander with Mill-Q water. *Hypnea musciformis* extract was then filtrated and collected. *Hypnea musciformis* extract was then dried at an oven to result extract powder. $AgNO_3$ and imidacloprid was purchased from Sigma-Aldrich. Any other chemicals were in analytical grade without further purification.

2.2. Biosynthesis of Ag NPs using Hypnea musciformis extract

Biosynthesis of Ag NPs was carried out using $AgNO_3$ and *Hypnea musciformis* extract as Ag precursor and reducing agent, respectively. Specifically, 0.5 g *Hypnea musciformis* extract was added into 10 mM $AgNO_3$ (20 mL) with 2 h sonication. The final solution turned from pale green to grey, indicating the formation of the Ag NPs. Centrifugation and water wash was used for removing excess *Hypnea musciformis* extract. The biosynthesized Ag NPs were collected after drying process.

2.3. Characterizations of biosynthesized Ag NPs

The morphology of the biosynthesized Ag NPs was characterized by a scanning electron microscopy (SEM, ZEISS X-MAX). Crystal information of the biosynthesized Ag NPs was collected form 10° to 80° in 2θ by a XRD (D8-Advance). The optical property of the biosynthesized Ag NPs was analysed by a UV-vis spectroscopy (Shimadzu UV-1601PC).

2.4. Electrochemical determination of imidacloprid

Biosynthesized Ag NPs was used for electrode surface modification. Typically, Glassy carbon electrode (GCE, 3 mm in diameter) was polished with 0.3 and 0.05 μm Al_2O_3 powder respectively and subsequently sonicated in ethanol and Mill-Q water to remove the physically adsorbed substance and dried in air. 5 μL of biosynthesized Ag NPs dispersion (1 mg/mL) was dropped on the GCE surface and dried at room temperature. Then, 5 μL of Nafion (1 wt% in ethanol) was dropped onto the Ag NPs/GCE and dried at room temperature. All electrochemical characterizations and determinations were carried out at a CHI 660E Electrochemical Workstation from Shanghai Chenhua Instrument (Shanghai, China) and conducted using a three-electrode system, with the modified GCE as working electrode, a platinum wire as the counter electrode, a saturated calomel electrode (SCE) as the reference electrode. All the measurements were carried out at room temperature. Electrochemical impedance spectroscopy (EIS) was used for characterizing the electrode resistance performance. 5 mM $[Fe(CN)_6]^{3-/4-}$ was used as probe, 0.1 M KCl was used as supporting electrolyte. Frequency range was set as 10^1 to 10^5 Hz and the amplitude was set as 5 mV. CV was performed in 0.1 M pH 7.0 PBS from -0.2 to -1.2 V at scan rate of 50 mV/s. DPV was also applied in 0.1 M pH 7.0 PBS from -0.5 to -1.2 V with a pulse amplitude of 50 mV and a pulse width of 50 ms.

3. RESULTS AND DISCUSSION

The successful formation of Ag NPs can be confirmed visually by the color change during the experiment. The morphology of the Ag NPs was firstly characterized using SEM. As shown in the Figure 1 A, the biosynthesized Ag NPs exhibited a small cluster morphology with sphere shape. No strong aggregation was observed probably due to the presence of bio-molecules on the Ag NPs surface. TEM was used for further characterizing the morphology of the biosynthesized Ag NPs

(Figure 1B). It can be seen that the formed Ag NPs showed a solid structure with average size diameter of 44 nm (based on 200 measurements of individual Ag NPs).

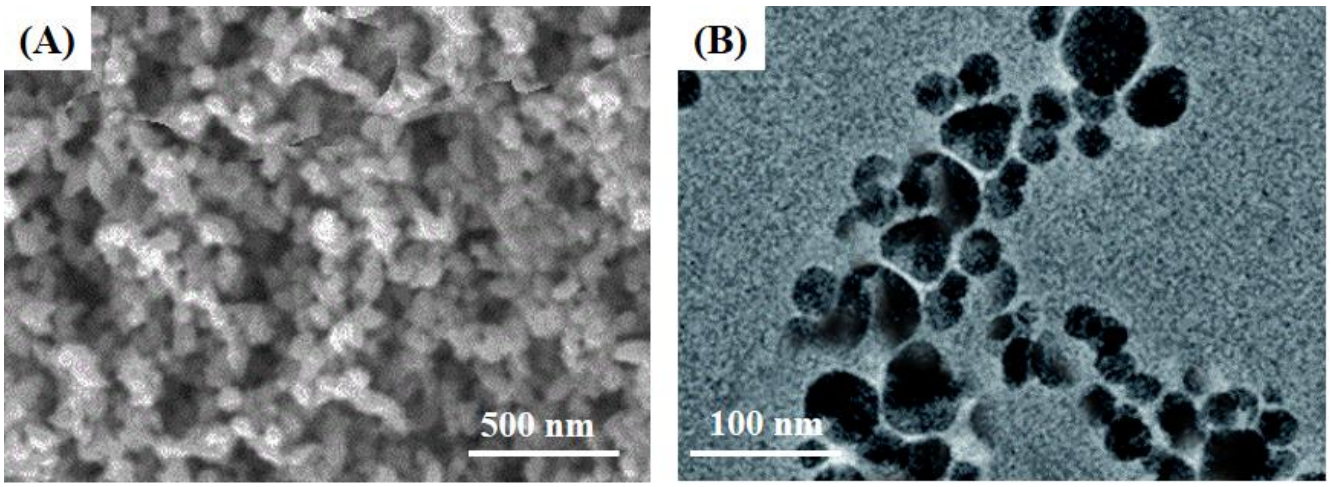

Figure 1. (A) SEM image and (B) TEM image of biosynthesized Ag NPs.

UV-vis spectrometer is a convenient instrument for determination of Ag NPs due to its surface plasmon resonance absorption. As shown in the Figure 2A, the UV-vis spectrum of the biosynthesized Ag NPs was recorded at the wavelength number range from 300 to 600 nm. A clear absorption band was observed centered at 450 nm, which associated with the biosynthesized Ag NPs [24].

The surface functional groups of biosynthesized Ag NPs was analyzed by FTIR. Figure 2B shows the FTIR spectrum of biosynthesized Ag NPs. A series of peaks were observed at 662, 697, 1031, 1640, 2956 and 3406 cm^{-1}, corresponding to the C–H band of alkene, (NH) C=O group the cage of cyclic peptides, C–N stretching vibration of aliphatic amines, N–H band of primary amines, C–H stretching of alkanes amide 1 band of proteins and O–H group in alcohols and phenols, respectively. The presence of these surface functional groups can highly improve the stability of the Ag NPs. Among these functional groups, the cyclic peptides could act as the reducing agent for $AgNO_3$ reduction. Moreover, according to previous studies, the reduction of $AgNO_3$ may also be contributed to the amino acids, fatty acids, vitamins, minerals, phenolic compounds and carbohydrates [25-27].

Crystal structure analysis of biosynthesized Ag NPs was carried out using a XRD. Figure 2C shows the XRD pattern of the biosynthesized Ag NPs. As shown in the figure, the diffraction peaks at 36.58°, 43.07°, 64.84°, and 77.61° can be assigned to the (200), (220), (311) and (222) silver face-centered-cube (fcc) crystal diffractions (JCPDS file no. 04-0783), respectively. No impurity peaks were observed in the XRD pattern, indicating no crystalized impurity was formed during the biosynthesis process. The crystallite size of the biosynthesized Ag NPs was calculated to be 12.7 nm according to the following equation:

$$D = 0.9\lambda / \beta \cos\theta$$

Where D is the crystalline size, λ is the wavelength of X-ray, β is the full width at half maximum light of maximum intensity peak and θ is the Bragg's angle.

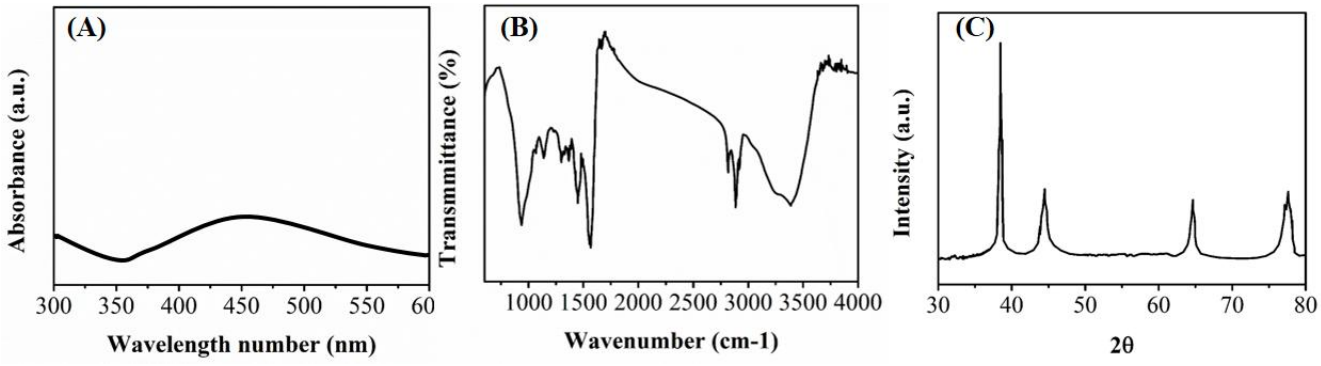

Figure 2. (A) UV-vis spectrum, (B) FTIR spectrum and (C) XRD pattern of biosynthesized Ag NPs.

EIS is a useful method for characterizing the electrode surface modification. The semicircle part observed at high frequencies in Nyquist plot is related to the charge transfer limiting process. Figure 3A shows the impedance spectra of bare GCE and biosynthesized Ag NPs modified GCE in the presence of 0.1 M KCl and 5 mM $[Fe(CN)_6]^{3-/4-}$. The charge transfer resistance value of bare GCE was determined as 745 Ω. The charge transfer resistance value increased dramatically after modification of biosynthesized Ag NPs due to the excellent electronic property of Ag NPs.

Electrochemistry property of bare GCE and biosynthesized Ag NPs modified GCE was studied by using $[Fe(CN)_6]^{3-/4-}$ as electrochemistry probe. Figure 3B shows the cyclic voltammograms (CV) of bare GCE and biosynthesized Ag NPs modified GCE in 0.1 M KCl and 5 mM $[Fe(CN)_6]^{3-/4-}$, at scan rate of 100 mV/s. It can be seen that the CV of bare GCE showed a pair of reversible redox peaks, corresponding to a one-electron electrochemical process of $Fe(CN)_6^{3-/4-}$. At the biosynthesized Ag NPs modified GCE, the redox current noticeably increased due to the superior conductivity and large surface area of Ag NPs.

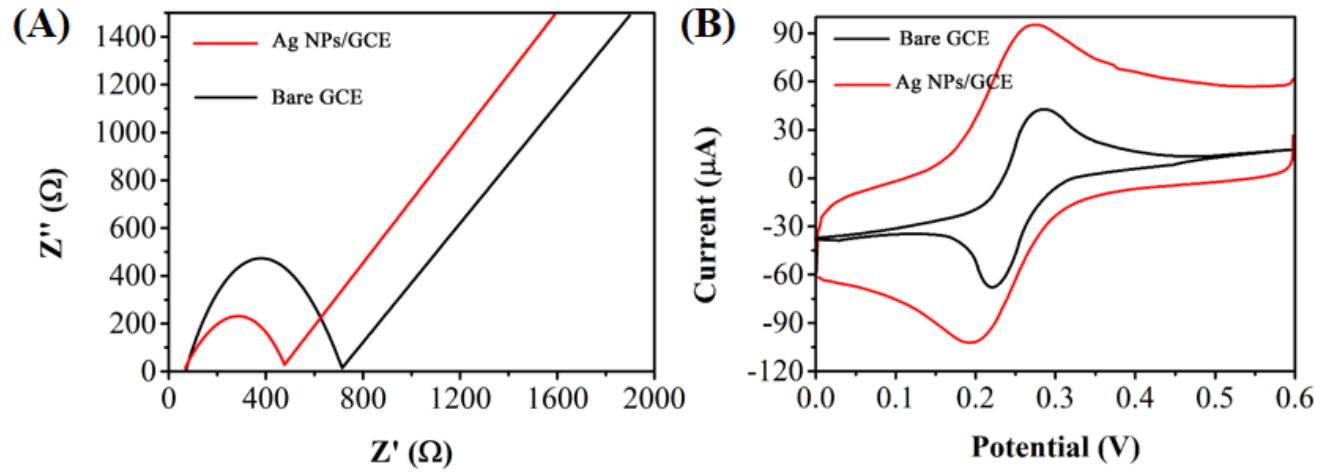

Figure 3. (A) Nyquist diagrams of bare GCE and biosynthesized Ag NPs modified GCE in 5 mM $K_4[Fe(CN)_6]$ + 0.1 M KCl.(B) CV for bare GCE and biosynthesized Ag NPs modified GCE in 5 mM $K_4[Fe(CN)_6]$ + 0.1 M KCl.

The electrochemical behaviours of bare GCE and biosynthesized Ag NPs modified GCE were investigated for a pesticide, 0.1 mM imidacloprid. Figure 4 shows the CV scan of bare GCE and biosynthesized Ag NPs modified GCE in PBS with 0.1 mM imidacloprid. Only a weak reduction peak was observed on the bare GCE caused by the electrochemical reduction of nitric group in imidacloprid [28, 29]. In contrast, the reduction peak currents of imidacloprid increased at biosynthesized Ag NPs modified GCE, which may be ascribed to the excellent superior conductivity and large surface area of biosynthesized Ag NPs. Moreover, the reduction peak showed a clear shift to more positive position, suggesting the Ag NPs also exhibited an excellent electrocatalytic reaction towards imidacloprid, which effectively reduced the reduction over potential.

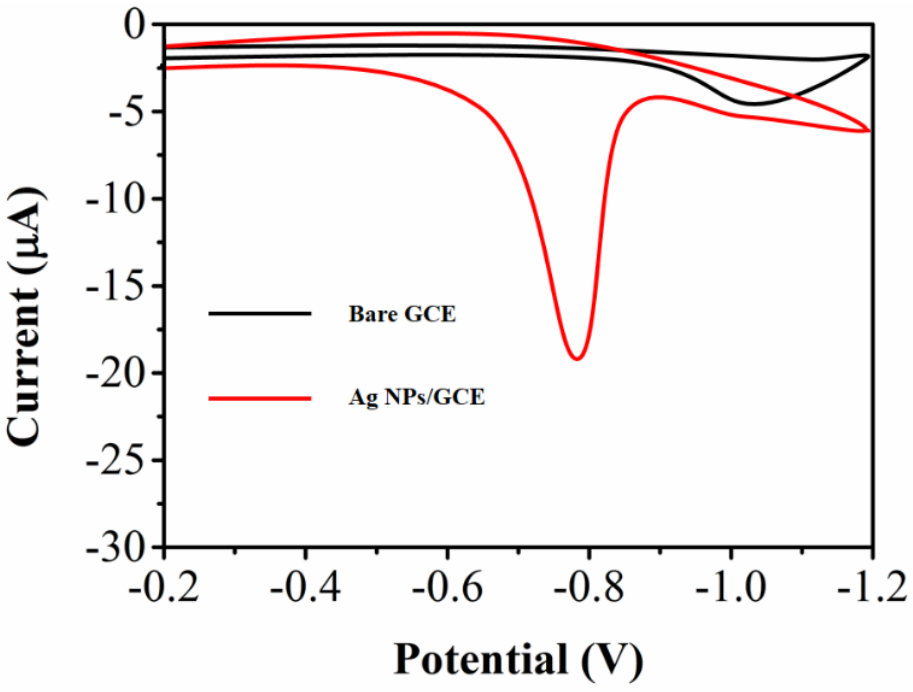

Figure 4. Cyclic voltammograms of bare GCE and biosynthesized Ag NPs modified GCE toward 100 μM imidacloprid in PBS (pH = 7) with scan rate of 50 mV/s.

The saturated adsorption capacity (Γ*) of imidacloprid at the biosynthesized Ag NPs modified GCE surface should be acquired. The chronocoulometry was a suitable technique, which was performed in PBS (pH 7.0) with absence and presence of 100 μM imidacloprid (Figure 5 A). Extracting data from Figure 5A, the corresponding relation of Q versus $t^{1/2}$ (oxidation process) showed good linear relationship with regression equations (Figure 5B) of Q (10^{-4} C)= 0.1422 $t^{1/2}$ + 1.0414 (R=0.998,) and Q (10^{-4} C) = 0.2124 $t^{1/2}$ + 1.853 (R=0.999). The two straight lines of the Q-$t^{1/2}$ were almost parallel in the presence and absence of imidacloprid, which indicating the adsorption-driven electrode process. Based on the intercept difference between two curves as well as the formula Q_{ads} = nFAΓ*, the value of Γ* was calculated to be 4.551 nM/cm^{-2}, which was the saturated adsorption capacity of imidacloprid at the biosynthesized Ag NPs modified GCE surface.

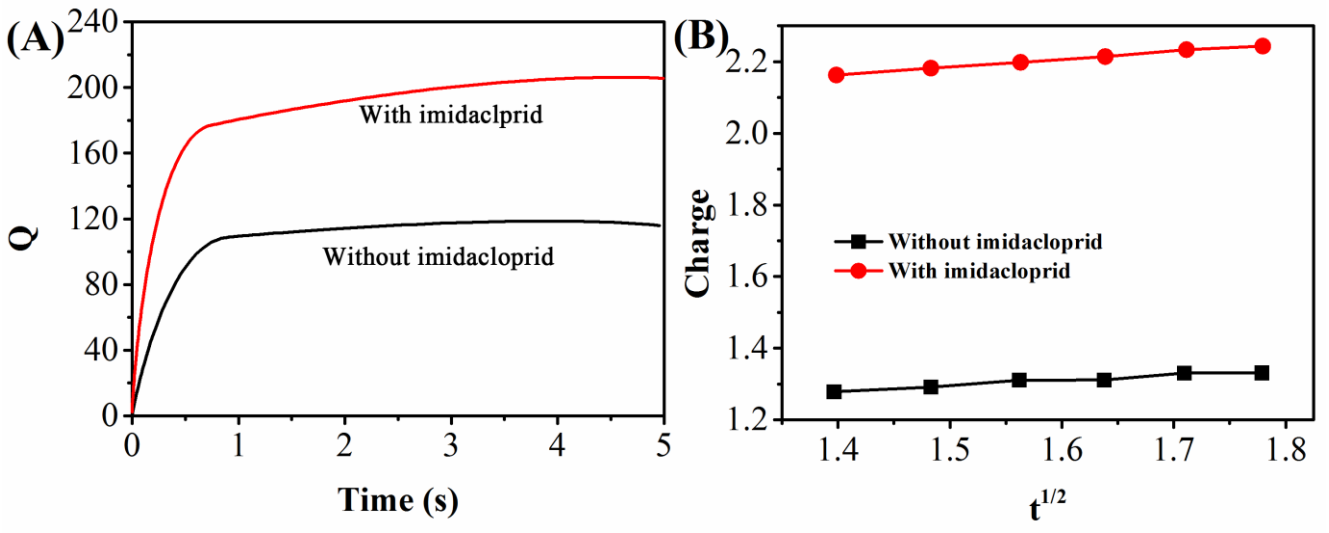

Figure 5. (A) Chronocoulometric response curves obtained in the absence and presence of 100 μM imidacloprid. (B) The relationship of charge Q (oxidation process) vs. $t^{1/2}$.

Differential pulse voltammetry (DPV) is an advance electrochemical method for capturing electrochemical signals on electrode surface.

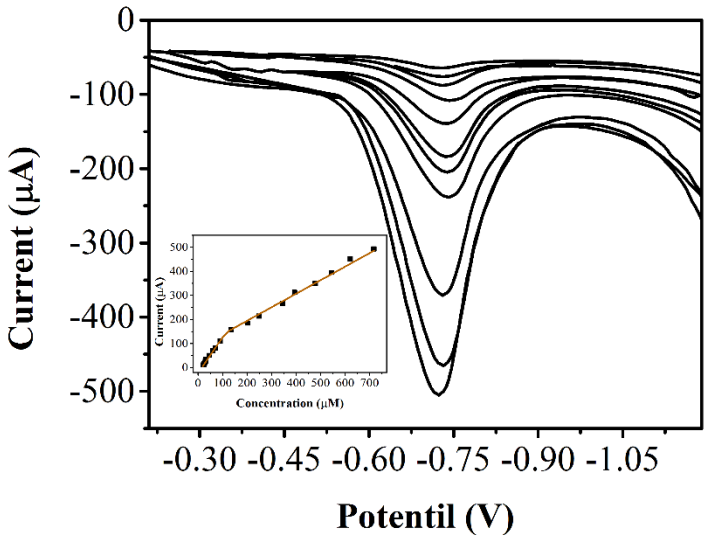

Figure 6. DPV profiles for the different concentrations of imidacloprid at biosynthesized Ag NPs modified GCE in PBS (pH=7). Inset: the calibration curve of imidacloprid.

Therefore, it is used here for detecting imidacloprid at low concentration. The DPV curves were recorded and present in Figure 5 A. It can be seen that the detection linear range of the biosynthesized Ag NPs modified GCE towards imidacloprid was divided into two parts. At low concentration of imidacloprid, a linear detection range was obtained at 0.05 to 80 μM. At high concentration of imidacloprid, a linear detection range was obtained at 100 to 750 μM. The detection limit of the proposed imidacloprid can be estimated as 0.02 μM based on the signal to noise of 3. This

analytical performance can be compared with those recently reported in the literature for Table 1. As compared with different modified electrodes, due to the high sensitivity of the proposed electrochemical performance, the biosynthesized Ag NPs/GCE exhibited two linear segments compared with other reports, which only contain one detection linear range. Moreover, due to the presence of biomolecule on the Ag NPs, which could prevent the poison of the electrode surface by imidacloprid especially at high concentration. Therefore, our proposed biosynthesized Ag NPs/GCE could used for detecting imidacloprid at high concentration condition.

Table 1. Comparison of our proposed imidacloprid electrochemical sensor with other reports.

Electrode	Linear range (μM)	Limit of detection (μM)	Reference
Bismuth film electrode	9.5-200	2.9	[30]
Carbon paste	6.7-117.4	2.04	[31]
GCE	10.9-1956	30.11	[32]
Prussian blue/MWNT/GCE	0.1-29.4	0.05	[33]
Ag NPs/TiO_2	0.5–3.5	0.25	[34]
DME	0.039–0.7828	0.01	[35]
HMDE	0.02-0.5 μM	0.02	[36]
Biosynthesized Ag NPs/GCE	0.05-80; 100-750	0.02	This work

In order to evaluate the real application ability, the biosynthesized Ag NPs modified GCE was applied for analyzing the imidacloprid in soil sample. Two soil samples were collected at farmland (with informed the land was spread imidacloprid two months ago) for testing. Table 2 displays the analyzed imidacloprid content determined by proposed electrochemical sensor. As shown in the table, the biosynthesized Ag NPs modified GCE showed good detection results. Therefore, we can claim that the biosynthesized Ag NPs modified GCE is capable for detecting imidacloprid in the real environmental samples.

Table 2. Determination of imidacloprid in soil samples using biosynthesized Ag NPs modified GCE.

Sample	Added (μM)	Found (μM)	Recovery (%)
Soil sample 1	0	1.25	—
	1	2.27	100.9
	5	6.32	101.6
	10	11.31	100.5
	20	21.31	100.3
Soil sample 2	0	2.29	—
	1	3.26	99.4
	5	7.24	99.3
	10	12.41	101.1
	20	22.32	100.1

4. CONCLUSION

In this communication, we reported a biosynthesis method for preparing Ag NPs using *Hypnea musciformis* extract as nature reducing agent. The biosynthesized Ag NPs showed a small cluster morphology with average size of 44 nm. FTIR study showed the presence of bio-molecules on the Ag NPs surface with prevent the strong aggregation. The biosynthesized Ag NPs were then used for commercial electrode surface modification and applied for pesticide, imidacloprid, determination. Moreover, the proposed imidacloprid electrochemical sensor was successfully used for detection imidacloprid in the real soil samples.

References

1. K. Hemath Naveen, G. Kumar, L. Karthik and K. Bhaskara Rao, *Arch. Appl. Sci. Res*, 2 (2010) 161
2. V. Mohanraj and Y. Chen, *Tropical Journal of Pharmaceutical Research*, 5 (2007) 561
3. (!!! INVALID CITATION !!!)
4. Y. Zheng, A. Wang, H. Lin, L. Fu and W. Cai, *RSC Advances*, 5 (2015) 15425
5. K. Rasmi, S. Vanithakumari, R. George, C. Mallika and U.K. Mudali, *Mater. Chem. Phys.*, 151 (2015) 133
6. L. Fu and A. Yu, *Nanoscience and Nanotechnology Letters*, 7 (2015) 147
7. L. Fu, S. Yu, L. Thompson and A. Yu, *RSC Advances*, 5 (2015) 40111
8. C. Yin, G. Lai, L. Fu, H. Zhang and A. Yu, *Electroanalysis*, 26 (2014) 409
9. C. Sarkar and H. Hirani, *International Journal of Scientific Engineering and Technology*, 4 (2015) 76
10. F. Mafuné, J.-y. Kohno, Y. Takeda, T. Kondow and H. Sawabe, *J Phys Chem B*, 104 (2000) 9111
11. D.L. Van Hyning and C.F. Zukoski, *Langmuir*, 14 (1998) 7034
12. M.A. Bhat, B. Nayak and A. Nanda, *Materials Today: Proceedings*, 2 (2015) 4395
13. H. Wang, X. Lang, R. Hao, L. Guo, J. Li, L. Wang and X. Han, *Nano Energy*, 19 (2016) 8
14. P. Yang, C. Jia, H. He, L. Chen and K. Matras-Postolek, *RSC Advances*, 5 (2015) 17210
15. R. Sathyavathi, M.B. Krishna, S.V. Rao, R. Saritha and D.N. Rao, *Advanced science letters*, 3 (2010) 138
16. R. Veerasamy, T.Z. Xin, S. Gunasagaran, T.F.W. Xiang, E.F.C. Yang, N. Jeyakumar and S.A. Dhanaraj, *Journal of Saudi Chemical Society*, 15 (2011) 113
17. K. Kalishwaralal, V. Deepak, S. Ram Kumar Pandian, M. Kottaisamy, S. BarathManiKanth, B. Kartikeyan and S. Gurunathan, *Colloids and Surfaces B: Biointerfaces*, 77 (2010) 257
18. V.C. Verma, R.N. Kharwar and A.C. Gange, *Nanomedicine*, 5 (2010) 33
19. M. Nizamuddin and A.C. Campbell, *Pakistan journal of botany*, 27 (1995) 257
20. V. Melo, D. Medeiros, F. Rios, L. Castelar and A. de FFU Carvalho, *Botanica Marina*, 40 (1997) 281
21. B. Das, *Indian Journal of Pharmacology*, 12 (1980) 259
22. J. Selvin and A.P. Lipton, *Journal of Marine Science and Technology*, 12 (2004) 1
23. K. Murugan, G. Benelli, S. Ayyappan, D. Dinesh, C. Panneerselvam, M. Nicoletti, J.-S. Hwang, P.M. Kumar, J. Subramaniam and U. Suresh, *Parasitology research*, 114 (2015) 2243
24. L. Fu, G. Lai, P.J. Mahon, J. Wang, D. Zhu, B. Jia, F. Malherbe and A. Yu, *RSC Advances*, 4 (2014) 39645
25. J.-I. Yang, C.-C. Yeh, J.-C. Lee, S.-C. Yi, H.-W. Huang, C.-N. Tseng and H.-W. Chang, *Molecules*, 17 (2012) 7241
26. K. Satyavani, S. Gurudeeban, T. Ramanathan and T. Balasubramanian, *J Nanobiotechnol*, 9 (2011) 2

27. S. Kansal, M. Singh and D. Sud, *J. Hazard. Mater.*, 153 (2008) 412
28. E. Giannakopoulos, P. Stivaktakis and Y. Deligiannakis, *Langmuir*, 24 (2008) 3955
29. Q. Shi and G. Diao, *Electrochimica Acta*, 58 (2011) 399
30. V. Guzsvány, M. Kádár, Z. Papp, L. Bjelica, F. Gaál and K. Toth, *Electroanalysis*, 20 (2008) 291
31. Z. Papp, I. Švancara, V. Guzsvány, K. Vytřas and F. Gaál, *Microchim. Acta.*, 166 (2009) 169
32. V.J. Guzsvány, F.F. Gaál, L.J. Bjelica and S.N. Ökrész, *Journal of the Serbian Chemical Society*, 70 (2005) 735
33. G.-d. Jin and X.-y. Hu, *Chinese Journal of Analysis Laboratory*, 27 (2008) 14
34. A. Kumaravel and M. Chandrasekaran, *Sensors and Actuators B: Chemical*, 158 (2011) 319
35. A. Navalón, R. El-Khattabi, A. González-Casado and J.L. Vilchez, *Microchim. Acta.*, 130 (1999) 261
36. A. Guiberteau, T. Galeano, N. Mora, P. Parrilla and F. Salinas, *Talanta*, 53 (2001) 943